IEEE Access
Multidisciplinary | Rapid Review | Open Access Journal

Received November 14, 2018, accepted November 21, 2018, date of publication November 29, 2018, date of current version December 27, 2018.

Digital Object Identifier 10.1109/ACCESS.2018.2884010

Secure Analog Network Coding With Wireless Energy Harvesting Under Multiple Eavesdroppers

KISONG LEE[1], (Member, IEEE), AND HYUN-HO CHOI[2], (Member, IEEE)
[1]School of Information and Communication Engineering, Chungbuk National University, Cheongju 28644, South Korea
[2]Department of Electrical, Electronic and Control Engineering, Hankyong National University, Anseong 17579, South Korea

Corresponding author: Hyun-Ho Choi (hhchoi@hknu.ac.kr)

This work was supported by the Basic Science Research Program through the National Research Foundation of Korea (NRF) funded by the Ministry of Science, ICT & Future Planning under Grant NRF-2016R1C1B1016261.

ABSTRACT In this paper, we consider a two-way relay system in which two users exchange data via a relay based on analog network coding (ANC) when multiple eavesdroppers exist. The relay replenishes energy from the two users' signal and utilizes it to forward the ANC signal to each user. Each user removes its own signal from the received signal through self-interference cancellation and decodes the desired data signal. On the other hand, the eavesdroppers overhear the relaying signal and attempt to recover the data of two users. For this ANC-based two-way relay network with multiple eavesdroppers, we propose two secure ANC protocols: power splitting-ANC (PS-ANC) and time switching-ANC (TS-ANC), in which the relay determines the power splitting ratio (α) and time switching ratio (β), respectively, to balance between the energy harvesting and the data reception. The optimal α and β for each protocol are obtained analytically to maximize the minimum achievable secrecy rate ($S_{\min}$) in consideration of multiple eavesdroppers. Analytical results show that both the PS-ANC and TS-ANC protocols with the optimal α and β accomplish the near-optimal $S_{\min}$ irrespective of the locations and number of eavesdroppers. The comparison of these two protocols in various network environments exhibits that PS-ANC has a better performance than TS-ANC when the network conditions are unfavorable for wiretapping by the eavesdroppers.

INDEX TERMS Analog network coding, energy harvesting, physical layer security, secrecy rate.

I. INTRODUCTION

Analog network coding (ANC) is an advanced spectral enhancement technique for two-way relay networks [1]. In this network scheme, two nodes simultaneously transmit their data signals to the relay in the first time slot. Then, the relay node forwards the superimposed version of these signals to the users in the second time slot. Each user can recover the desired signal from the relaying signal by subtracting its original signal through the self-interference cancellation (SIC) technique. This operation can increase spectral efficiency up to double compared to the traditional routing approach, so the ANC has received attention as an attractive technology for future relay networks [2].

In wireless communications, security is a critical issue because wireless channels are inherently vulnerable to eavesdropping. In the two-way relay network using ANC, the relay is more likely to be attacked by eavesdroppers due to its intermediate position between two information sources [3]. Therefore, the combination of ANC and physical layer security (PLS) technique has been considered for secure relaying [4]–[8]. Zhang *et al.* [4] analyzed the security capacity of ANC system considering external and internal eavesdroppers and verified that ANC can improve the PLS performance in the two-way relay channel. Sunny *et al.* [5] proposed a scheme to improve the secrecy rate of cooperative networks using ANC, which maximizes the average secrecy rate between the source and the destination subject to an overall power budget. Deng *et al.* [6] suggested a PLS enhancement scheme in ANC systems based on artificial noise and showed that the proposed scheme greatly improves the ergodic secrecy capacity compared with beamforming scheme. Wang *et al.* [7], [8] proposed a two-phase ANC and power allocation scheme for the constituent nodes to enhance the security of the data exchange with the help of multiple relay nodes in the presence of an eavesdropper.

In addition, energy scarcity and energy efficiency are another major challenges in relay networks because the relay consumes additional power for signal processing and relaying [9]. One of the latest technologies to address this issue is wireless energy harvesting (EH). The relay can replenish energy from external radio frequency (RF) signals by using EH techniques and this energy is used for relay operation effectively [10]. Since RF radiation can convey information as well as energy at the same time, simultaneous wireless information and power transfer (SWIPT) technology has been widely applied to relay networks [11]–[16]. Nasir *et al.* [11] first applied the time switching and power splitting techniques to a relay network for enabling both energy harvesting and information processing at the relay. Chen *et al.* [12] analyzed the performances of SWIPT-based two-way relaying protocol in terms of the ergodic capacity and outage probability, and discovered the diversity-multiplexing tradeoff. Tutuncuoglu *et al.* [13] presented a hybrid relaying protocol that changes the relaying strategy according to instantaneous transmission powers in order to maximize sum rate. Fang *et al.* [14] designed the transceiver of relay for distributed energy beamforming-based SWIPT in a two-way relay system. Ju *et al.* [15] analyzed an optimal coefficient of power splitting for wireless-powered relay to maximize the end-to-end throughput of ANC network. Modem and Prakriya [16] investigated the performances of ANC with respect to ergodic sum-rate, system outage, and symbol error rate when the relay with EH had a single antenna and the sources had multiple antennas.

Up to date, the studies on either PLS or EH in ANC-based relay networks have been conducted mainly, but recently the secure ANC network considering both PLS and EH has begun to be addressed. Lee *et al.* [17], [18] considered a wireless-powered relay and proposed adaptive power-splitting and time-switching relay protocols to maximize secrecy capacity. However, [17] is limited to one-way relay and considers only a single eavesdropper and [18] requires an additional jammer and direct channels from users to eavesdropper for operation. Therefore, there is still a need for study on two-way ANC networks considering both PLS and EH in more practical network environments. Unlike [17] and [18], we propose secure ANC protocols in a new network topology where a two-way relay receives both wireless energy and jamming signal from both sources and multiple eavesdroppers exist around the vulnerable relay. More specifically, two users want to exchange data with each other through a two-way relay with EH while multiple eavesdroppers try to overhear the relaying signal. The relay replenishes energy from some portion of the received signals and uses this harvested energy to forward the ANC signal without the consumption of the relay's own energy. Each user removes its own signal from the relaying signal using an SIC technique and then decodes the desired data signal. Under this operation, we optimize the ratio of energy harvesting at the relay based on power splitting and time switching techniques to maximize the minimum achievable secrecy rate.

The main contributions of this paper are as follows. First, we present a two-way relay system model when the relay performs both EH and ANC and it is exposed to multiple eavesdroppers, and then solve the optimization problem that maximizes the minimum achievable secrecy rate ($S_{\min}$). Second, we suggest two secure ANC protocols: *power splitting-ANC (PS-ANC)* and *time switching-ANC (TS-ANC)*. These protocols determine the ratio of energy harvesting from the received source signals based on power splitting and time switching, respectively, in consideration of information leakage to eavesdroppers. Third, we prove the concavity of secrecy rate for each user with respect to the power splitting ratio (α) and time switching ratio (β) in high signal-to-noise ratio (SNR) environments, and then obtain the closed-form expressions of the optimal α^* for PS-ANC and the optimal β^* for TS-ANC to maximize $S_{\min}$. Last, our analysis result provides insights for understanding the behaviors of the proposed ANC protocols. Specifically, the optimal ratios (α^*, β^*) and the corresponding secrecy rates are not affected by channel gains of the relay-eavesdropper links. This enables us to achieve the near-optimal performance of $S_{\min}$ no matter how many eavesdroppers exist anywhere. In addition, the comparison of PS-ANC and TS-ANC shows that they can complement each other according to the mode of network deployment.

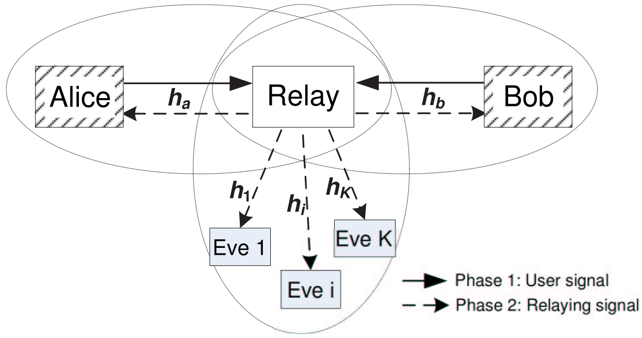

FIGURE 1. Considered ANC-based two-way relay network with multiple eavesdroppers.

The rest of this paper is organized as follows. In Section II, we present the system model of the considered ANC-based two-way relay network. In Section III, we propose PS-ANC protocol and derive the optimal power splitting ratio to maximize the minimum achievable secrecy rate. On the other hand, in Section IV, TS-ANC protocol is proposed and the optimal time switching ratio is obtained to maximize the minimum achievable secrecy rate. In Section V, we evaluate the performance of PS-ANC and TS-ANC protocols and compare their behaviors in various scenarios. Finally, we present our concluding remarks in Section VI.

II. SYSTEM DESCRIPTION

Figure 1 describes the considered ANC-based two-way relay network with multiple eavesdroppers. There are two users (i.e., Alice and Bob), a relay, and multiple eavesdroppers (denoted as Eve). Specifically, there are K Eves randomly distributed around the relay to wiretap the vulnerable relaying signal. The channels for Alice-to-Relay, Bob-to-Relay, and Relay-to-i^{th} Eve are denoted as h_a, h_b, and h_i for $i \in \{1, \cdots, K\}$, respectively, assuming that the channel between two entities is reciprocal [12], [13]. Here, direct links between Alice or Bob and Eves are ignored by assuming that Alice and Bob can identify the existence of Eves in other many ways [19]–[21]. In addition, a quasi-static channel fading is considered, thus the channel maintains constant over one coherence interval and varies separately in different coherence intervals [21]. The noises at Alice, Bob, relay, and Eves are denoted as n_a, n_b, n_r, and n_e, respectively, and they all follow an additive white Gaussian noise (AWGN) with zero-mean and variance σ^2, i.e., $n_a = n_b = n_r = n_e \sim \mathcal{CN}\left(0, \sigma^2\right)$.

The considered secure ANC protocols using EH operate in two phases. At the first phase, Alice and Bob transmit their own signals, x_a and x_b, to the relay at the same time. Here, we assume that the relay has no internal power source or does not consume its own power for relaying so that it harvests energy from the received information signals during this phase [12]–[14]. This is quite reasonable in a practical environment that does not use a dedicated relay because any node acting as a relay will not want to waste its energy for relaying. Thus, the relay harvests energy from the received signals for some portion (power or time) of the first phase while receiving information for the other portion of the phase. To perform this energy harvesting and information processing simultaneously, the relay selectively uses a power splitting [22] or time switching scheme [23]. It is assumed that there is no constraint on the minimum power level for harvesting energy [11]. Thereafter, the two received information signals are combined by a basic ANC scheme [1].

At the second phase, the relay broadcasts the combined ANC signal to both users based on the amplify-and-forward technique by using the energy harvested during the first phase. Here, we assume that all the harvested energy is used for this transmission. Upon receiving the signal from the relay, Alice and Bob can acquire the desired data signal from the received relay signal by SIC technique. Here, we suppose that the SIC is perfect in order to focus on the upper bound performance of the proposed ANC protocol [24]–[26]. On the other hand, at the second phase, multiple Eves around the relay receive the relaying signal and attempt to decode the information of Alice and Bob. By the way, each user signal prevents Eves from decoding another user signal because the relaying signal includes both x_a and x_b by the ANC operation.

III. POWER SPLITTING-ANALOG NETWORK CODING

A. PROTOCOL MODEL

Figure 2 depicts the frame structure and operation of PS-ANC. The frame has a length of T and is divided into two phases of equal length (i.e., $\frac{T}{2}$) [11], [22]. During the first phase, the relay harvests energy and receives data from the received user signals, x_a and x_b, at the same time using a power splitting method [22]. In other words, a portion α of the received RF signals is used for harvesting energy and a portion $(1-\alpha)$ of the received RF signals is utilized for receiving information, subject to $0 \le \alpha \le 1$. Then, the received signal at the relay y_r is expressed as

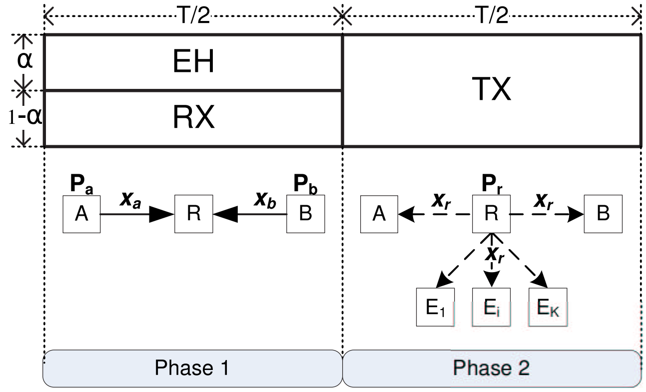

FIGURE 2. Frame structure and operation of PS-ANC.

$$y_r = \sqrt{(1-\alpha)P_a}h_a x_a + \sqrt{(1-\alpha)P_b}h_b x_b + n_r \quad (1)$$

where P_a and P_b are the transmission powers of Alice and Bob, respectively, and x_a and x_b have a normalized power, such as $\mathbb{E}[|x_a|^2] = \mathbb{E}[|x_b|^2] = 1$. From this, the harvested energy at the relay, $\mathcal{E}_h$, is given by

$$\mathcal{E}_h = \frac{T}{2}\eta\alpha(P_a|h_a|^2 + P_b|h_b|^2) = \frac{T\eta\alpha\mathcal{E}_r}{2} \quad (2)$$

where $0 < \eta < 1$ is the energy harvesting efficiency and $\mathcal{E}_r$ is defined as $P_a|h_a|^2 + P_b|h_b|^2$.

During the second phase with $\frac{T}{2}$, the relay performs ANC and forwards the combined ANC signal using the harvested energy, $\mathcal{E}_h$. This transmitting signal at the relay, x_r, is represented by

$$\begin{aligned} x_r &= \frac{\sqrt{P_r}y_r}{\sqrt{(1-\alpha)(P_a|h_a|^2 + P_b|h_b|^2) + \sigma^2}} \\ &= \frac{\sqrt{P_r}y_r}{\sqrt{(1-\alpha)\mathcal{E}_r + \sigma^2}} \end{aligned} \quad (3)$$

where P_r is the transmission power at the relay, which is obtained from

$$P_r = \frac{\mathcal{E}_h}{T/2} = \eta\alpha\mathcal{E}_r. \quad (4)$$

Then, the received signal at Alice, y_a, is expressed as

$$\begin{aligned} y_a &= h_a x_r + n_a \\ &= \frac{\sqrt{(1-\alpha)P_b P_r}h_a h_b x_b + \sqrt{P_r}h_a n_r}{\sqrt{(1-\alpha)\mathcal{E}_r + \sigma^2}} \\ &\quad + \underbrace{\frac{\sqrt{(1-\alpha)P_a P_r}h_a^2 x_a}{\sqrt{(1-\alpha)\mathcal{E}_r + \sigma^2}}}_{\text{SIC}} + n_a \\ &= \frac{\sqrt{(1-\alpha)P_b P_r}h_a h_b x_b + \sqrt{P_r}h_a n_r}{\sqrt{(1-\alpha)\mathcal{E}_r + \sigma^2}} + n_a. \end{aligned} \quad (5)$$

Similarly, the received signal at Bob, y_b, is expressed as

$$y_b = h_b x_r + n_b = \frac{\sqrt{(1-\alpha)P_a P_r} h_a h_b x_a + \sqrt{P_r} h_b n_r}{\sqrt{(1-\alpha)\mathcal{E}_r + \sigma^2}} + \underbrace{\frac{\sqrt{(1-\alpha)P_b P_r} h_b^2 x_b}{\sqrt{(1-\alpha)\mathcal{E}_r + \sigma^2}}}_{\text{SIC}} + n_b = \frac{\sqrt{(1-\alpha)P_a P_r} h_a h_b x_a + \sqrt{P_r} h_b n_r}{\sqrt{(1-\alpha)\mathcal{E}_r + \sigma^2}} + n_b. \quad (6)$$

Note that in (5) and (6), each user can eliminate the self-interference part related to its own signal, i.e., $\frac{\sqrt{(1-\alpha)P_a P_r} h_a^2 x_a}{\sqrt{(1-\alpha)\mathcal{E}_r + \sigma^2}}$ and $\frac{\sqrt{(1-\alpha)P_b P_r} h_b^2 x_b}{\sqrt{(1-\alpha)\mathcal{E}_r + \sigma^2}}$, by SIC. On the other hand, the received signal at the i^{th} Eve, y_i, is represented by

$$y_i = h_i x_r + n_e = \frac{\sqrt{(1-\alpha)P_a P_r} h_a h_i x_a + \sqrt{(1-\alpha)P_b P_r} h_b h_i x_b}{\sqrt{(1-\alpha)\mathcal{E}_r + \sigma^2}} + \frac{\sqrt{P_r} h_i n_r}{\sqrt{(1-\alpha)\mathcal{E}_r + \sigma^2}} + n_e, \quad i \in \{1, \cdots, K\}. \quad (7)$$

From (5), the SNR at Alice for receiving Bob's signal (x_b), Γ_a, is obtained as

$$\Gamma_a = \frac{\frac{(1-\alpha)P_b P_r |h_a|^2 |h_b|^2}{(1-\alpha)\mathcal{E}_r + \sigma^2}}{\frac{P_r |h_a|^2 \sigma^2}{(1-\alpha)\mathcal{E}_r + \sigma^2} + \sigma^2} = \frac{\eta\alpha(1-\alpha)\mathcal{E}_r P_b |h_a|^2 |h_b|^2}{\eta\alpha\mathcal{E}_r |h_a|^2 \sigma^2 + \sigma^2((1-\alpha)\mathcal{E}_r + \sigma^2)}. \quad (8)$$

From (6), the SNR at Bob for receiving Alice's signal (x_a), Γ_b, is expressed as

$$\Gamma_b = \frac{\frac{(1-\alpha)P_a P_r |h_a|^2 |h_b|^2}{(1-\alpha)\mathcal{E}_r + \sigma^2}}{\frac{P_r |h_b|^2 \sigma^2}{(1-\alpha)\mathcal{E}_r + \sigma^2} + \sigma^2} = \frac{\eta\alpha(1-\alpha)\mathcal{E}_r P_a |h_a|^2 |h_b|^2}{\eta\alpha\mathcal{E}_r |h_b|^2 \sigma^2 + \sigma^2((1-\alpha)\mathcal{E}_r + \sigma^2)}. \quad (9)$$

To combine (8) and (9), we set $j \in \{a, b\}$ and denote $\backslash j = b$ if $j = a$ and $\backslash j = a$ if $j = b$. Using this, the SNR at Alice or Bob is reformulated as

$$\Gamma_j = \frac{\eta\alpha(1-\alpha)\mathcal{E}_r P_{\backslash j} |h_j|^2 |h_{\backslash j}|^2}{\eta\alpha\mathcal{E}_r |h_j|^2 \sigma^2 + \sigma^2((1-\alpha)\mathcal{E}_r + \sigma^2)}, \quad j \in \{a, b\}. \quad (10)$$

Then, the achievable rate at Alice or Bob is given by $R_j = \frac{T}{2}\log_2(1 + \Gamma_j)$ for $j \in \{a, b\}$.

On the other hand, from (7), the SNR at the i^{th} Eve for detecting x_b destined for Alice, Γ_a^i, is calculated as

$$\Gamma_a^i = \frac{\frac{(1-\alpha)P_b P_r |h_b|^2 |h_i|^2}{(1-\alpha)\mathcal{E}_r + \sigma^2}}{\frac{(1-\alpha)P_a P_r |h_a|^2 |h_i|^2}{(1-\alpha)\mathcal{E}_r + \sigma^2} + \frac{P_r |h_i|^2 \sigma^2}{(1-\alpha)\mathcal{E}_r + \sigma^2} + \sigma^2} = \frac{\eta\alpha(1-\alpha)\mathcal{E}_r P_b |h_b|^2 |h_i|^2}{\eta\alpha\mathcal{E}_r |h_i|^2((1-\alpha)P_a |h_a|^2 + \sigma^2) + \sigma^2((1-\alpha)\mathcal{E}_r + \sigma^2)}. \quad (11)$$

Moreover, the SNR at the i^{th} Eve for detecting x_a destined for Bob, Γ_b^i, is calculated as

$$\Gamma_b^i = \frac{\frac{(1-\alpha)P_a P_r |h_a|^2 |h_i|^2}{(1-\alpha)\mathcal{E}_r + \sigma^2}}{\frac{(1-\alpha)P_b P_r |h_b|^2 |h_i|^2}{(1-\alpha)\mathcal{E}_r + \sigma^2} + \frac{P_r |h_i|^2 \sigma^2}{(1-\alpha)\mathcal{E}_r + \sigma^2} + \sigma^2} = \frac{\eta\alpha(1-\alpha)\mathcal{E}_r P_a |h_a|^2 |h_i|^2}{\eta\alpha\mathcal{E}_r |h_i|^2((1-\alpha)P_b |h_b|^2 + \sigma^2) + \sigma^2((1-\alpha)\mathcal{E}_r + \sigma^2)}. \quad (12)$$

Combining (11) and (12), the SNR at the i^{th} Eve destined for Alice ($j = a$) or Bob ($j = b$) is reexpressed as

$$\Gamma_j^i = \frac{\eta\alpha(1-\alpha)\mathcal{E}_r P_{\backslash j} |h_{\backslash j}|^2 |h_i|^2}{\eta\alpha\mathcal{E}_r |h_i|^2((1-\alpha)P_j |h_j|^2 + \sigma^2) + \sigma^2((1-\alpha)\mathcal{E}_r + \sigma^2)}, \quad j \in \{a, b\}, \quad i \in \{1, 2, \cdots, K\} \quad (13)$$

where $\backslash j = b$ if $j = a$ and $\backslash j = a$ if $j = b$. Then, the achievable rate at the i^{th} Eve is obtained as $R_j^i = \frac{T}{2}\log_2(1 + \Gamma_j^i)$ for $j \in \{a, b\}$ and $i \in \{1, 2, \cdots, K\}$.

B. MAXIMIZING THE MINIMUM ACHIEVABLE SECRECY RATE

The secrecy rate at Alice or Bob when i^{th} Eve overhears x_b or x_a destined for Alice or Bob is defined as

$$S_j^i \triangleq \left[R_j - R_j^i\right]^+, \quad j \in \{a, b\}, \ i \in \{1, 2, \cdots, K\} \quad (14)$$

where $[\cdot]^+ = \max(0, \cdot)$. From the fact that there are K eavesdropping links for each user, the minimum achievable secrecy rate for Alice or Bob is given by $S_j \triangleq \min_i \left\{S_j^i\right\}$ for $j \in \{a, b\}$. Finally, the minimum achievable secrecy rate for both users is expressed as [19], [20]

$$S_{\min} \triangleq \min_j \{S_j\} = \min_j \min_i \left\{\left[R_j - R_j^i\right]^+\right\} = \min_j \left\{\left[R_j - \max_i\{R_j^i\}\right]^+\right\}$$

$$= \min_j \left\{ \left[R_j - R_j^{i_j^*} \right]^+ \right\}$$
$$= \min_j \left\{ \left[\frac{T}{2} \log_2 \left(\frac{1+\Gamma_j}{1+\Gamma_j^{i_j^*}} \right) \right]^+ \right\}, \quad j \in \{a,b\} \quad (15)$$

where $R_j^{i_j^*} = \max_i \{R_j^i\}$ and $i_j^* = \arg\max_i \{R_j^i\}$ for each $j \in \{a,b\}$. In other words, Eve i_j^* denotes the one with the largest achievable rate for wiretapping $s_{\setminus j}$ destined for Alice ($j=a$) or Bob ($j=b$). In the high SNR regime, $S_{\min}$ can be approximated as

$$S_{\min} \approx \min_j \left\{ \left[\frac{T}{2} \log_2 \left(\frac{\Gamma_j}{\Gamma_j^{i_j^*}} \right) \right]^+ \right\}, \quad j \in \{a,b\}. \quad (16)$$

Note that EH is generally available in high SNR environments because of its low sensitivity [27], therefore, our assumption is reasonable. The effect of the high SNR approximation on performance will be discussed in subsection V-A.

Our objective is to derive the optimal power splitting ratio α^* that maximizes $S_{\min}$. Under the assumption of high SNR, we try to find the optimal value of α that maximizes (16), that is alternatively represented by

$$\alpha^* = \arg\max_\alpha \left\{ \min_j \left\{ \frac{\Gamma_j}{\Gamma_j^{i_j^*}} \right\} \right\}, \quad j \in \{a,b\}. \quad (17)$$

Thus, we define (18), shown at the bottom of this page, where $A_j = \eta \mathcal{E}_r P_j |h_{i_j^*}|^2 |h_j|^2$, $B_j = \mathcal{E}_r(\eta |h_{i_j^*}|^2 - 1)\sigma^2$, $C_j = \mathcal{E}_r(\eta |h_j|^2 - 1)\sigma^2$, and $D = \sigma^2(\mathcal{E}_r + \sigma^2)$.

To find the value of α_j for maximizing each $\Gamma_{S,j}$, we first prove the concavity of $\Gamma_{S,j}$.

Proposition 1 (Concavity): $\Gamma_{S,j}$ is concave with respect to (w.r.t.) α_j subject to $0 \le \alpha_j \le 1$.

Proof: The second derivative of $\Gamma_{S,j}$ w.r.t. α_j is

$$\frac{\partial^2 \Gamma_{S,j}}{\partial \alpha_j^2} = -\frac{2|h_j|^2 D\{A_j(C_j+D) + C_j(B_j - C_j)\}}{|h_{i_j^*}|^2 (\alpha_j C_j + D)^3}. \quad (19)$$

There is no doubt that $A_j(C_j+D)$ and $(\alpha_j C_j + D)$ are positive. Moreover, $A_j(C_j+D) + C_j(B_j - C_j) > 0$ independent of the sign of $C_j(B_j - C_j)$ because $A_j(C_j+D)$ has order σ^2 while $C_j(B_j-C_j)$ has order σ^4. In consequence, the condition, $\frac{\partial^2 \Gamma_{S,j}}{\partial \alpha_j^2} < 0$, holds and then $\Gamma_{S,j}$ is concave w.r.t. α_j. ■

From Proposition 1, we suggest Proposition 2.

Proposition 2 (Optimal Power Splitting Ratio): The optimal power splitting ratio (α_j^*) for maximizing $\Gamma_{S,j}$ for $j \in \{a,b\}$ is given by

$$\alpha_j^* = \frac{-A_j D + \sqrt{A_j D\{A_j(C_j+D) + C_j(B_j - C_j)\}}}{A_j C_j}, \quad j \in \{a,b\}. \quad (20)$$

Proof: From the first derivative of $\Gamma_{S,j}$ w.r.t. α_j, we can build the following condition.

$$\frac{\partial \Gamma_{S,j}}{\partial \alpha_j} = -\frac{|h_j|^2\{A_j C_j \alpha_j^2 + 2A_j D \alpha_j - (A_j + B_j - C_j)D\}}{|h_{i_j^*}|^2 (\alpha_j C_j + D)^2} = 0. \quad (21)$$

Then, the solutions of (21) can be derived as

$$\alpha_{j,\pm} = \frac{-A_j D \pm \sqrt{A_j D\{A_j(C_j+D) + C_j(B_j - C_j)\}}}{A_j C_j}. \quad (22)$$

In (22), $C_j < 0$ since $\eta|h_j|^2 < 1$ in C_j. Thus, the following inequality, $A_j(C_j+D) < A_j D$, holds. Moreover, $A_j(C_j+D)$ is greater than $|C_j(B_j - C_j)|$ as discussed in (19). This represents that $\sqrt{A_j D\{A_j(C_j+D) + C_j(B_j - C_j)\}}$ has a value between 0 and $A_j D$. In addition, $\alpha_{j,-} > 1$ because $|D| > |C_j|$ and $C_j < 0$, while $0 < \alpha_{j,+} < 1$. As a result, $\alpha_{j,+}$ can be decided as α_j^*. ■

Lemma 1: In the high SNR regime, the optimal power splitting ratio, α_j^*, is not influenced by the relay-to-Eves channel, h_i.

Proof: Under the assumption of high SNR, we can eliminate the equations with order σ^4. Therefore, $C_j(B_j - C_j)$ becomes zero and $D \approx \sigma^2 \mathcal{E}_r$ so that α_j^* in (20) can be simplified as

$$\begin{aligned} \alpha_j^* &\approx \frac{-A_j D + \sqrt{A_j D\{A_j(C_j+D)\}}}{A_j C_j} \\ &= \frac{-D + \sqrt{D(C_j+D)}}{C_j} \\ &\approx \frac{-\sigma^2 \mathcal{E}_r + \sqrt{\sigma^2 \mathcal{E}_r(\mathcal{E}_r(\eta|h_j|^2 - 1)\sigma^2 + \sigma^2 \mathcal{E}_r)}}{\mathcal{E}_r(\eta|h_j|^2 - 1)\sigma^2} \\ &= \frac{1}{1+\sqrt{\eta|h_j|^2}}, \quad j \in \{a,b\}. \end{aligned} \quad (23)$$

■

Lemma 1 implies that α_j^* can be optimized for each user by only the information related to h_a or h_b without any

$$\begin{aligned} \Gamma_{S,j} &\triangleq \frac{\Gamma_j}{\Gamma_j^{i_j^*}} \\ &= \frac{|h_j|^2 \left\{ \eta\alpha\mathcal{E}_r |h_{i_j^*}|^2 ((1-\alpha)P_j|h_j|^2 + \sigma^2) + \sigma^2((1-\alpha)\mathcal{E}_r + \sigma^2) \right\}}{|h_{i_j^*}|^2 \left\{ \eta\alpha\mathcal{E}_r |h_j|^2 \sigma^2 + \sigma^2((1-\alpha)\mathcal{E}_r + \sigma^2) \right\}} \\ &= \frac{|h_j|^2\{-\alpha^2 A_j + \alpha(A_j + B_j) + D\}}{|h_{i_j^*}|^2\{\alpha C_j + D\}} \end{aligned} \quad (18)$$

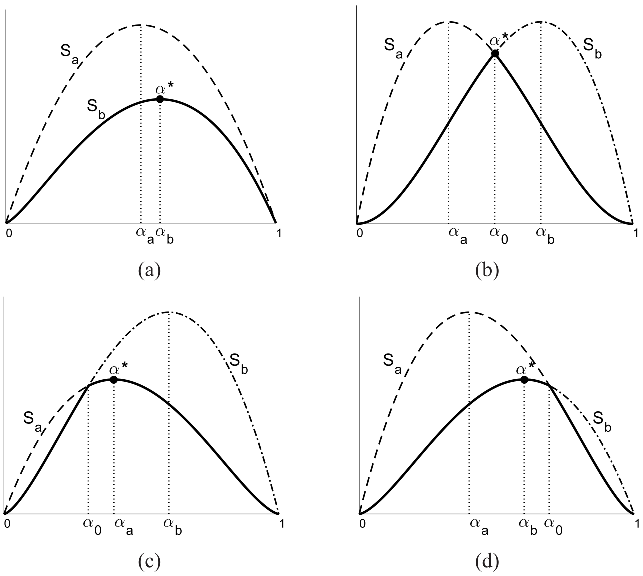

FIGURE 3. All scenarios for determining α^*. (a) When $\alpha_0^* = 0$ or 1. (b) When $(\alpha_a^* - \alpha_0^*)(\alpha_b^* - \alpha_0^*) \leq 0$. (c) When $(\alpha_a^* - \alpha_0^*)(\alpha_b^* - \alpha_0^*) > 0$ and $S_a(\alpha_a^*) \leq S_b(\alpha_b^*)$. (d) When $(\alpha_a^* - \alpha_0^*)(\alpha_b^* - \alpha_0^*) > 0$ and $S_a(\alpha_a^*) > S_b(\alpha_b^*)$.

knowledge about channel information to Eves (i.e., h_i). Thus, PS-ANC can be effectively operated in real environments because it is not always known where Eves are located. In short, α_j^* can be obtained from knowledge of h_j for $j \in \{a, b\}$ in a high SNR regime.

From the result of Proposition 2, the optimal α^* for maximizing $\min\{S_a, S_b\}$ can be determined. Note that S_j is derived directly from $\Gamma_{S,j}$ for high SNR. There exists α_0^* that keeps $\Gamma_{S,a} = \Gamma_{S,b}$ such that α_j^* and α_0^* should be considered jointly. Figure 3 shows four scenarios for determining α^*: (a) If there is no crossover point that holds $S_a = S_b$ (i.e., $\alpha_0^* = 0$ or 1), α_j^* that achieves smaller S_j is selected as α^*. (b) When α_0^* lies between α_a^* and α_b^* (i.e., $(\alpha_a^* - \alpha_0^*)(\alpha_b^* - \alpha_0^*) \leq 0$), α_0^* is chosen as α^*. (c) and (d) When α_0^* is smaller or larger than both α_a^* and α_b^* (i.e., $(\alpha_a^* - \alpha_0^*)(\alpha_b^* - \alpha_0^*) > 0$), α_j^* that accomplishes a smaller S_j is chosen as α^*.

Then, α_0^* can be derived as follows. It is clear that $C_j \approx -\mathcal{E}_r\sigma^2$ because $\eta|h_j|^2 \ll 1$ in C_j. Therefore, the denominator of $\Gamma_{S,j}$ can be approximated as $|h_{i_j^*}|^2\{\alpha C_j + D\} \approx |h_{i_j^*}|^2(1-\alpha)\mathcal{E}_r\sigma^2$. Then, we can build (24), shown at the bottom of this page, from $\Gamma_{S,a} = \Gamma_{S,b}$. Using the quadratic formula, the solution of (24) can be derived as in (25), shown at the bottom of this page. Note that $\alpha_\pm$ indicates the crossover point where $\Gamma_{S,a} = \Gamma_{S,b} = \Gamma_S$, in other words, $S_a = S_b = S$. Comparing S at α_+ with that at α_-, α_0^* is selected to achieve a larger S, as follows.

$$\alpha_0^* = \begin{cases} \alpha_+ & \text{if } S(\alpha_+) \geq S(\alpha_-), \\ \alpha_- & \text{if } S(\alpha_+) < S(\alpha_-). \end{cases} \tag{26}$$

Considering α_j^* and α_0^* jointly, the optimal power splitting ratio for maximizing $\min\{S_a, S_b\}$ is finally determined as

$$\alpha^* = \begin{cases} \alpha_0^* & \text{if } (\alpha_a^* - \alpha_0^*)(\alpha_b^* - \alpha_0^*) \leq 0, \\ \alpha_a^* & \text{if } (\alpha_a^* - \alpha_0^*)(\alpha_b^* - \alpha_0^*) > 0 \\ & \quad \text{and } S_a(\alpha_a^*) \leq S_b(\alpha_b^*), \\ \alpha_b^* & \text{if } (\alpha_a^* - \alpha_0^*)(\alpha_b^* - \alpha_0^*) > 0 \\ & \quad \text{and } S_a(\alpha_a^*) > S_b(\alpha_b^*). \end{cases} \tag{27}$$

IV. TIME SWITCHING-ANALOG NETWORK CODING

A. PROTOCOL MODEL

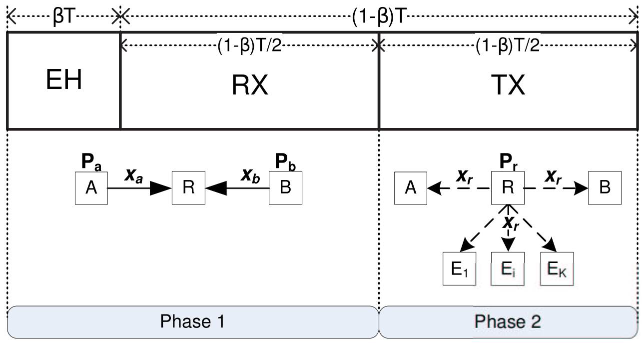

FIGURE 4. Frame structure and operation of TS-ANC.

Figure 4 depicts the frame structure and operation of TS-ANC. The frame consists of two phases according to the functionality of the relay, e.g., reception or transmission. The first phase for reception is divided into two subphases. The first subphase with the duration of βT is utilized for harvesting energy, and the second subphase with the duration of $\frac{(1-\beta)T}{2}$ is used for receiving information from the user signals. On the other hand, during the second phase with the duration of $\frac{(1-\beta)T}{2}$, the relay transmits the received signal to the users using the harvested energy [11].

The harvested energy at the relay, $\mathcal{E}_h$, is given by

$$\mathcal{E}_h = \eta\beta T(P_a|h_a|^2 + P_b|h_b|^2) = \eta\beta T\mathcal{E}_r \tag{28}$$

$$\begin{aligned} 0 &= (|h_{i_a^*}|^2|h_b|^2A_b - |h_{i_b^*}|^2|h_a|^2A_a)\alpha^2 + (|h_{i_b^*}|^2|h_a|^2(A_a + B_a) - |h_{i_a^*}|^2|h_b|^2(A_b + B_b))\alpha + D(|h_{i_b^*}|^2|h_a|^2 - |h_{i_a^*}|^2|h_b|^2) \\ &\approx (|h_{i_a^*}|^2|h_b|^2A_b - |h_{i_b^*}|^2|h_a|^2A_a)\alpha^2 + (|h_{i_b^*}|^2|h_a|^2A_a - |h_{i_a^*}|^2|h_b|^2A_b)\alpha + D(|h_{i_b^*}|^2|h_a|^2 - |h_{i_a^*}|^2|h_b|^2). \end{aligned} \tag{24}$$

$$\alpha_\pm = \min\left[\max\left[\frac{1}{2} \pm \sqrt{\frac{1}{4} - \frac{(|h_a|^2/|h_{i_a^*}|^2 - |h_b|^2/|h_{i_b^*}|^2)\sigma^2}{\eta(P_b|h_b|^4 - P_a|h_a|^4)}}, 0\right], 1\right]. \tag{25}$$

where $\mathcal{E}_r$ is defined as $P_a|h_a|^2 + P_b|h_b|^2$. The received signal at the relay, y_r, is represented by

$$y_r = \sqrt{P_a}h_a x_a + \sqrt{P_b}h_b x_b + n_r. \tag{29}$$

Then, the transmitted signal from the relay, x_r, using $\mathcal{E}_h$ is expressed as

$$x_r = \frac{\sqrt{P_r}y_r}{\sqrt{P_a|h_a|^2 + P_b|h_b|^2 + \sigma^2}} = \frac{\sqrt{P_r}y_r}{\sqrt{\mathcal{E}_r + \sigma^2}} \tag{30}$$

where the transmission power at the relay, P_r, is defined as

$$P_r = \frac{\mathcal{E}_h}{(1-\beta)T/2} = \frac{2\eta\beta\mathcal{E}_r}{1-\beta}. \tag{31}$$

Then, the received signal at Alice, y_a, is expressed as

$$\begin{aligned} y_a &= h_a x_r + n_a \\ &= \frac{\sqrt{P_b P_r}h_a h_b x_b + \sqrt{P_r}h_a n_r}{\sqrt{\mathcal{E}_r + \sigma^2}} + \underbrace{\frac{\sqrt{P_a P_r}h_a^2 x_a}{\sqrt{\mathcal{E}_r + \sigma^2}}}_{\text{SIC}} + n_a \\ &= \frac{\sqrt{P_b P_r}h_a h_b x_b + \sqrt{P_r}h_a n_r}{\sqrt{\mathcal{E}_r + \sigma^2}} + n_a. \end{aligned} \tag{32}$$

Moreover, the received signal at Bob, y_b, is expressed as

$$\begin{aligned} y_b &= h_b x_r + n_b \\ &= \frac{\sqrt{P_a P_r}h_a h_b x_a + \sqrt{P_r}h_b n_r}{\sqrt{\mathcal{E}_r + \sigma^2}} + \underbrace{\frac{\sqrt{P_b P_r}h_b^2 x_b}{\sqrt{\mathcal{E}_r + \sigma^2}}}_{\text{SIC}} + n_b \\ &= \frac{\sqrt{P_a P_r}h_a h_b x_a + \sqrt{P_r}h_b n_r}{\sqrt{\mathcal{E}_r + \sigma^2}} + n_b. \end{aligned} \tag{33}$$

Similar to the PS-ANC protocol, each user can eliminate its self-interference part, i.e., $\frac{\sqrt{P_a P_r}h_a^2 x_a}{\sqrt{\mathcal{E}_r+\sigma^2}}$ and $\frac{\sqrt{P_b P_r}h_b^2 x_b}{\sqrt{\mathcal{E}_r+\sigma^2}}$, by SIC. On the other hand, the received signal at the eavesdropper E_i, y_i, is given by

$$\begin{aligned} y_i &= h_i x_r + n_e \\ &= \frac{\sqrt{P_a P_r}h_a h_i x_a + \sqrt{P_b P_r}h_b h_i x_b}{\sqrt{\mathcal{E}_r + \sigma^2}} + \frac{\sqrt{P_r}h_i n_r}{\sqrt{\mathcal{E}_r + \sigma^2}} + n_e. \end{aligned} \tag{34}$$

From (32) and (33), the SNR at Alice or Bob, Γ_j, is found as

$$\begin{aligned} \Gamma_j &= \frac{\frac{2\eta\beta\mathcal{E}_r P_{\setminus j}|h_j|^2|h_{\setminus j}|^2}{(1-\beta)(\mathcal{E}_r+\sigma^2)}}{\frac{2\eta\beta\mathcal{E}_r|h_j|^2\sigma^2}{(1-\beta)(\mathcal{E}_r+\sigma^2)} + \sigma^2} \\ &= \frac{2\eta\beta\mathcal{E}_r P_{\setminus j}|h_j|^2|h_{\setminus j}|^2}{2\eta\beta\mathcal{E}_r|h_j|^2\sigma^2 + \sigma^2(1-\beta)(\mathcal{E}_r+\sigma^2)}, \quad j \in \{a, b\} \end{aligned} \tag{35}$$

where $\setminus j = b$ if $j = a$ and $\setminus j = a$ if $j = b$. Then, the achievable rate at Alice or Bob is expressed as $R_j = \frac{(1-\beta)T}{2}\log_2(1+\Gamma_j)$ for $j \in \{a, b\}$. Moreover, from (34), the SNR at the i^{th} Eve for detecting $s_{\setminus j}$ transmitted to Alice ($j = a$) or Bob ($j = b$), Γ_j^i, is represented by

$$\begin{aligned} \Gamma_j^i &= \frac{\frac{2\eta\beta\mathcal{E}_r P_{\setminus j}|h_{\setminus j}|^2|h_i|^2}{(1-\beta)(\mathcal{E}_r+\sigma^2)}}{\frac{2\eta\beta\mathcal{E}_r P_j|h_j|^2|h_i|^2}{(1-\beta)(\mathcal{E}_r+\sigma^2)} + \frac{2\eta\beta\mathcal{E}_r|h_i|^2\sigma^2}{(1-\beta)(\mathcal{E}_r+\sigma^2)} + \sigma^2} \\ &= \frac{2\eta\beta\mathcal{E}_r P_{\setminus j}|h_{\setminus j}|^2|h_i|^2}{2\eta\beta\mathcal{E}_r|h_i|^2(P_j|h_j|^2+\sigma^2) + \sigma^2(1-\beta)(\mathcal{E}_r+\sigma^2)}. \end{aligned} \tag{36}$$

Then, the achievable rate at the i^{th} Eve is expressed as $R_j^i = \frac{(1-\beta)T}{2}\log_2(1+\Gamma_j^i)$ for $j \in \{a, b\}$ and $i \in \{1, 2, \cdots, K\}$.

B. MAXIMIZING THE MINIMUM ACHIEVABLE SECRECY RATE

The minimum achievable secrecy rate is formulated as

$$\begin{aligned} S_{\min} &\triangleq \min_j \{S_j\} \\ &= \min_j \min_i \left\{\left[R_j - R_j^i\right]^+\right\} \\ &= \min_j \left\{\left[R_j - \max_i\{R_j^i\}\right]^+\right\} \\ &= \min_j \left\{\left[R_j - R_j^{i_j^*}\right]^+\right\} \\ &= \min_j \left\{\left[\frac{(1-\beta)T}{2}\log_2\left(\frac{1+\Gamma_j}{1+\Gamma_j^{i_j^*}}\right)\right]^+\right\} \end{aligned} \tag{37}$$

$$\approx \min_j \left\{\left[\frac{(1-\beta)T}{2}\log_2\left(\frac{\Gamma_j}{\Gamma_j^{i_j^*}}\right)\right]^+\right\}, \quad j \in \{a, b\} \tag{38}$$

where the approximation is obtained by the assumption of high SNR.

We try to find the optimal time switching ratio β^* that maximizes $S_{\min}$. Thus, the optimal β^* is given by

$$\beta^* = \arg\max_\beta \left\{\min_j \left\{\left[\frac{(1-\beta)T}{2}\log_2\left(\frac{\Gamma_j}{\Gamma_j^{i_j^*}}\right)\right]^+\right\}\right\}, \quad j \in \{a, b\}. \tag{39}$$

Here, we define $\Gamma_{S,j}$ as

$$\begin{aligned} \Gamma_{S,j} &\triangleq \frac{\Gamma_j}{\Gamma_j^{i_j^*}} \\ &= \frac{|h_j|^2\{2\eta\beta\mathcal{E}_r|h_{i_j^*}|^2(P_j|h_j|^2+\sigma^2) + \sigma^2(1-\beta)(\mathcal{E}_r+\sigma^2)\}}{|h_{i_j^*}|^2\{2\eta\beta\mathcal{E}_r|h_j|^2\sigma^2 + \sigma^2(1-\beta)(\mathcal{E}_r+\sigma^2)\}} \\ &= \frac{|h_j|^2((F_j - D)\beta + D)}{|h_{i_j^*}|^2((G_j - D)\beta + D)} \end{aligned} \tag{40}$$

where $F_j = 2\eta\mathcal{E}_r|h_{i_j^*}|^2(P_j|h_j|^2+\sigma^2)$, $G_j = 2\eta\mathcal{E}_r|h_j|^2\sigma^2$, and $D = \sigma^2(\mathcal{E}_r+\sigma^2)$. Now, we prove the concavity of S_j w.r.t. β_j to derive the optimal β_j^* for maximizing each S_j.

Proposition 3 (Concavity): S_j is concave w.r.t. β_j subject to $0 \le \beta_j \le 1$ in the high SNR regime.

Proof: We define $h_j(\beta_j) \triangleq f(\beta_j)r_j(\beta_j)$, where $h_j(\beta_j) \triangleq S_j$, $f(\beta_j) \triangleq \frac{(1-\beta_j)T}{2}$, and $r_j(\beta_j) \triangleq \log_2(\Gamma_{S,j})$. Then, the second derivative of $h_j(\beta_j)$ w.r.t. β_j can be derived as

$$\begin{aligned} h_j''(\beta_j) &= f''(\beta_j)r_j(\beta_j) + 2f'(\beta_j)r_j'(\beta_j) + f(\beta_j)r_j''(\beta_j) \\ &= 2f'(\beta_j)r_j'(\beta_j) + f(\beta_j)r_j''(\beta_j). \quad (\because f''(\beta_j)=0) \end{aligned} \tag{41}$$

Here, $f'(\beta_j)$, $r_j'(\beta_j)$, and $r_j''(\beta_j)$ are calculated as

$$\begin{aligned} f'(\beta_j) &= -\frac{T}{2}, \\ r_j'(\beta_j) &= \frac{D(F_j-G_j)}{\ln 2X_jY_j}, \\ r_j''(\beta_j) &= \frac{-D(F_j-G_j)\{(G_j-D)X_j+(F_j-D)Y_j\}}{\ln 2X_j^2Y_j^2}, \end{aligned} \tag{42}$$

where $X_j = (F_j-D)\beta_j + D$ and $Y_j = (G_j-D)\beta_j + D$. Therefore, $h_j''(\beta_j)$ is represented by (43), shown at the bottom of the next page.

Since the following conditions, $F_j > G_j$ and $F_j > D$, hold under the assumption of high SNR, we can conclude that $h''(\beta_j) < 0$ and S_j is concave w.r.t. β_j for $0 \le \beta_j \le 1$. ■

From Proposition 3, we can present the following proposition.

Proposition 4 (Optimal Time Switching Ratio): In the high SNR regime, the optimal time switching ratio (β_j^*) for maximizing S_j for $j \in \{a,b\}$ is given by

$$\beta_j^* = \frac{1}{\mathbb{W}\left(\frac{2\eta|h_j|^2(P_j|h_j|^2+\sigma^2)}{\sigma^2\cdot e}\right)+1}, \quad j\in\{a,b\} \tag{44}$$

where $\mathbb{W}(\cdot)$ denotes the Lambert W-function.

Proof: Based on Proposition 3, we can find the optimal β_j^* for maximizing S_j from the first derivative of S_j w.r.t. β_j, as follows.

$$\begin{aligned} &\frac{\partial S_j}{\partial \beta_j} \\ &= \frac{T}{2\ln 2}\left[\frac{F_j}{(F_j-D)\beta_j+D} - \frac{\Theta_j}{(\Theta_j-D)\beta_j+D} - \ln\frac{|h_j|^2}{|h_{i_j^*}|^2}\right. \\ &\quad \left. - \ln\left\{(F_j-D)\beta_j+D\right\} + \ln\left\{(\Theta_j-D)\beta_j+D\right\}\right] = 0. \end{aligned} \tag{45}$$

With the assumption of high SNR, the conditions, $F_j \gg D$, $F_j \gg \Theta_j$, and $D \gg \Theta_j$, can hold. Therefore, (45) is transformed to

$$\frac{\partial S_j}{\partial \beta_j} = \frac{1}{\beta_j} + \ln\frac{1-\beta_j}{\beta_j} - \ln\frac{F_j|h_j|^2}{D|h_{i_j^*}|^2} = 0. \tag{46}$$

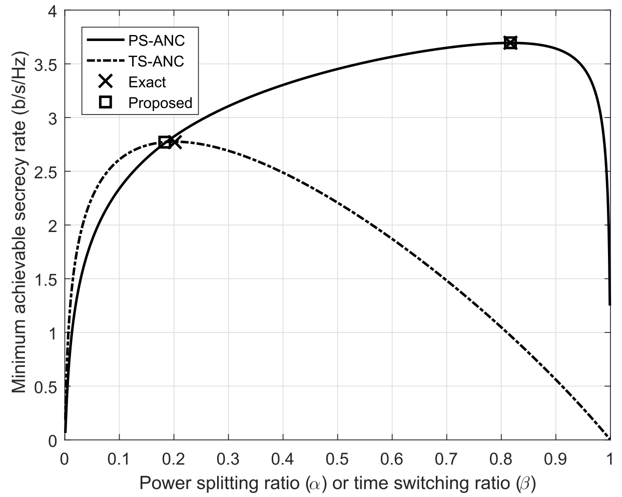

FIGURE 5. Minimum achievable secrecy rate vs. power splitting ratio or time switching ratio.

By solving (46), the optimal β_j^* is derived as

$$\beta_j^* = \frac{1}{\mathbb{W}\left(\frac{2\eta\mathcal{E}_r|h_{i_j^*}|^2(P_j|h_j|^2+\sigma^2)|h_j|^2}{\sigma^2(\mathcal{E}_r+\sigma^2)|h_{i_j^*}|^2\cdot e}\right)+1} \tag{47}$$

$$\approx \frac{1}{\mathbb{W}\left(\frac{2\eta|h_j|^2(P_j|h_j|^2+\sigma^2)}{\sigma^2\cdot e}\right)+1}. \tag{48}$$

■

Note that similar to the PS-ANC, β_j^* is only affected by h_j for $j \in \{a,b\}$ in high SNR environments. In other words, the TS-ANC can also operate using the channel information of h_j, regardless of the knowledge of channel information on Eves (i.e., h_i).

Furthermore, we need to jointly consider β_j^* and β_0^* that satisfy $\Gamma_{S,a} = \Gamma_{S,b}$ to find the optimal β^* to maximize $\min\{S_a, S_b\}$ in high SNR. To find β_0^*, we use the fact that $D \approx \mathcal{E}_r\sigma^2$ and $G_j \ll D$ because $2\eta|h_j|^2 \ll 1$ in G_j. Therefore, the denominator of $\Gamma_{S,j}$ can be approximated as $|h_{i_j^*}|^2((G_j-D)\beta+D) \approx |h_{i_j^*}|^2(1-\beta)\mathcal{E}_r\sigma^2$. Then, we can build (49), shown at the bottom of the next page, from $\Gamma_{S,a} = \Gamma_{S,b}$ in the high SNR assumption.

In (49), the approximation holds because $2\eta\mathcal{E}_r|h_{i_j^*}|^2\sigma^2$ can be neglected in $F_j - D$ from the fact that $2\eta|h_{i_j^*}|^2\mathcal{E}_r\sigma^2 \ll \mathcal{E}_r\sigma^2$. Then, the solution of (49) can be found as

$$\beta_0^* = \min\left[\max\left[\frac{1}{1+\frac{2\eta(P_a|h_a|^4-P_b|h_b|^4)}{\left(|h_b|^2/|h_{i_b^*}|^2-|h_a|^2/|h_{i_a^*}|^2\right)\sigma^2}}, 0\right], 1\right]. \tag{50}$$

Similar to the PS-ANC protocol, in consideration of β_j^* and β_0^*, the optimal time switching ratio for maximizing

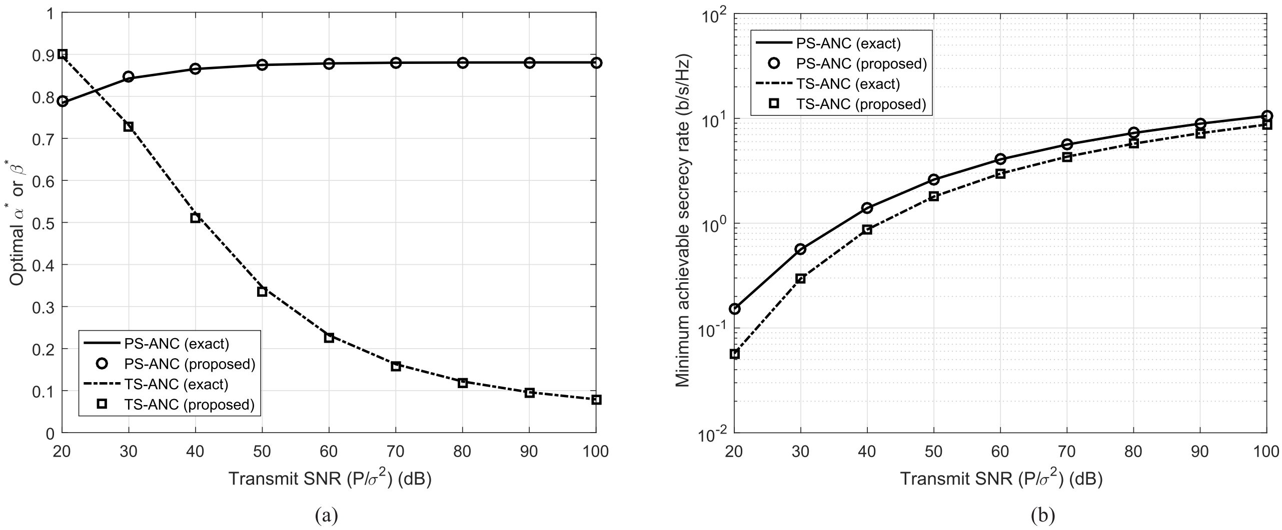

FIGURE 6. Performances against transmit SNR. (a) Power splitting ratio or time switching ratio versus transmit SNR. (b) Minimum achievable secrecy rate versus transmit SNR.

$\min\{S_a, S_b\}$ is finally determined as

$$\beta^* = \begin{cases} \beta_0^* & \text{if } (\beta_a^* - \beta_0^*)(\beta_b^* - \beta_0^*) \le 0, \\ \beta_a^* & \text{if } (\beta_a^* - \beta_0^*)(\beta_b^* - \beta_0^*) > 0 \\ & \quad \text{and } S_a(\beta_a^*) \le S_b(\beta_b^*), \\ \beta_b^* & \text{if } (\beta_a^* - \beta_0^*)(\beta_b^* - \beta_0^*) > 0 \\ & \quad \text{and } S_a(\beta_a^*) > S_b(\beta_b^*). \end{cases} \quad (51)$$

V. RESULTS AND DISCUSSION

To evaluate the proposed PS-ANC and TS-ANC protocols, we first investigate the optimality of the obtained α and β, and then compare the two protocols in diverse scenarios.

A. VERIFICATION OF OPTIMALITY

To demonstrate the optimality of the proposed α^* and β^*, the following parameters are utilized as default; $T = 1$, $P_a = P_b = P = 1$, $\sigma^2 = 10^{-5}$, $K = 10$, and $\eta = 0.5$ [28].

Figure 5 shows the minimum achievable secrecy rate ($S_{\min}$) versus the power splitting ratio (α) or the time switching ratio (β). Here, we set $|h_a|^2 = |h_b|^2 = 0.1$ and generate $|h_i|^2$ randomly from 0.08 to 0.12 for each i. Note that the exact α^* and β^* are the optimal solutions found by exhaustive search to maximize (15) and (37), respectively, without the high SNR assumption, while the proposed α^* and β^* are the analytical results obtained from (27) and (51), respectively, with the high SNR assumption. It is shown that $S_{\min}$ is concave w.r.t. both α and β so that the exact α^* and β^* for maximizing $S_{\min}$ exist. It is also clearly shown that the proposed α^* and β^* are well matched to the exact α^* and β^*, respectively.

Figure 6 shows (a) the optimal α^* or β^* and (b) the minimum achievable secrecy rate versus the transmit SNR ($\frac{P}{\sigma^2}$), respectively. Here, we used an exponential random variable with a mean of 0.1 to generate h_a, h_b, and h_i. Figure 6(a) shows that α^* increases slightly while β^* decreases as SNR increases. This indicates that it is advantageous for the relay to use a large amount of the received power for harvesting energy in the PS-ANC protocol while it is beneficial for the relay to use much of the time for receiving and forwarding data in the TS-ANC protocol. As shown in Figure 6(a), in spite of the high SNR assumption, the proposed α^* (or β^*) coincides with the exact α^* (or β^*) for all SNR regimes. Moreover, as shown in Figure 6(b), there is little difference in $S_{\min}$ between the proposed α^* (or β^*) and the exact α^* (or β^*) in either protocol.

B. PERFORMANCE COMPARISONS

We compare the minimum achievable secrecy rate of the PS-ANC and TS-ANC protocols depending on variations of wireless channel and other factors considering realistic

$$h_j''(\beta_j) = \frac{-TD(F_j - G_j)\left\{\left(\left(\frac{1+\beta_j}{2}\right)G_j + \left(\frac{1-\beta_j}{2}\right)D\right)X_j + \frac{1-\beta_j}{2}(F_j - D)Y_j\right\}}{\ln 2 X_j^2 Y_j^2}. \quad (43)$$

$$\begin{aligned} 0 &= \{|h_{i_a^*}|^2|h_b|^2(F_b - D) - |h_{i_b^*}|^2|h_a|^2(F_a - D)\}\beta + (|h_{i_a^*}|^2|h_b|^2 - |h_{i_b^*}|^2|h_a|^2)D \\ &\approx \{|h_{i_a^*}|^2|h_b|^2(2\eta\mathcal{E}_r P_b|h_{i_b^*}|^2|h_b|^2 - \mathcal{E}_r\sigma^2) - |h_{i_b^*}|^2|h_a|^2(2\eta\mathcal{E}_r P_a|h_{i_a^*}|^2|h_a|^2 - \mathcal{E}_r\sigma^2)\}\beta + (|h_{i_a^*}|^2|h_b|^2 - |h_{i_b^*}|^2|h_a|^2)\mathcal{E}_r\sigma^2. \end{aligned} \quad (49)$$

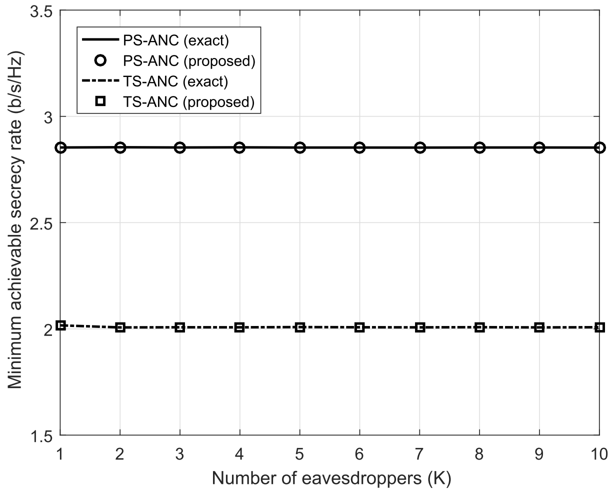

FIGURE 7. **Minimum achievable secrecy rate vs. number of eavesdroppers (K) when d_{ab} = 200 m and $d_a = d_b$ = 100 m.**

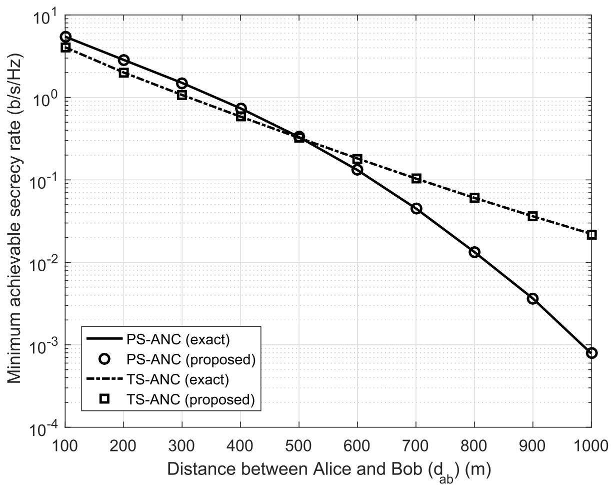

FIGURE 8. **Minimum achievable secrecy rate vs. distance between Alice and Bob (d_{ab}) when $d_a = \frac{d_{ab}}{2}$.**

environments. The following system parameters are used as default: $T = 1$, $\eta = 0.5$, $K = 10$, $P_a = P_b = P = 43$ dBm, and $\sigma^2 = -97$ dBm [29]. Eavesdroppers are uniformly located at a distance between 10 m and 100 m from the relay. The wireless channels for Alice-to-Relay, Bob-to-Relay, and Relay-to-i^{th} Eve are defined as $h_a = f_a(d_a)^{-m}$, $h_b = f_b(d_b)^{-m}$, and $h_i = f_i(d_i)^{-m}$ for $i \in \{1, \cdots, K\}$, respectively. Here, $d_{\{\cdot\}}$ denotes the physical distance between two corresponding nodes and $f_{\{\cdot\}}$ denotes a fading coefficient that follows the Exponential distribution with mean $\lambda_{\{\cdot\}}$. We set $\lambda_a = \lambda_b = \lambda_i = 1$ and $m = 2.7$ for an urban cellular network environment [30].

1) EFFECTS OF WIRELESS CHANNELS

First, we reveal the effects of channel variations on the performance. Figure 7 shows the minimum achievable secrecy rate versus the number of eavesdroppers (K) when the distance between Alice and Bob (d_{ab}) is set at 200 m and the distance between each user and relay (d_a and d_b) is set at 100 m. The result shows that PS-ANC achieves the constant

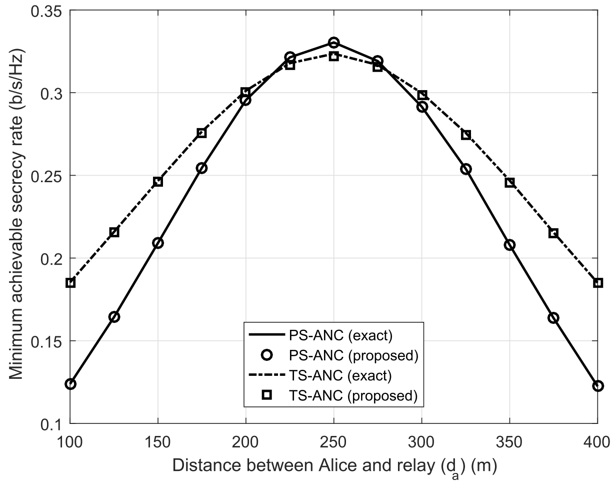

FIGURE 9. **Minimum achievable secrecy rate vs. distance between Alice and relay (d_a) when d_{ab} = 500 m.**

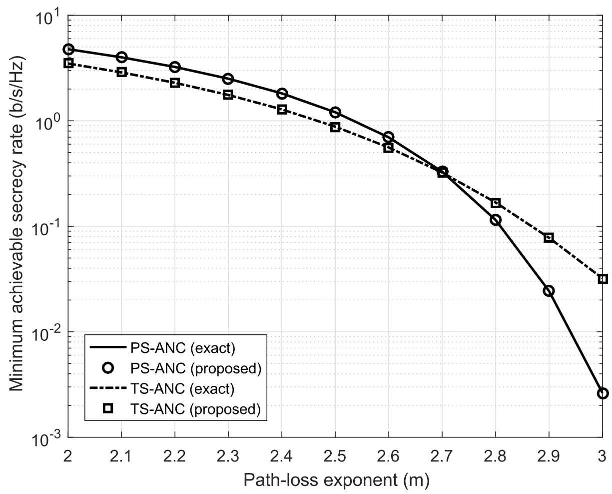

FIGURE 10. **Minimum achievable secrecy rate vs. path-loss exponent (m).**

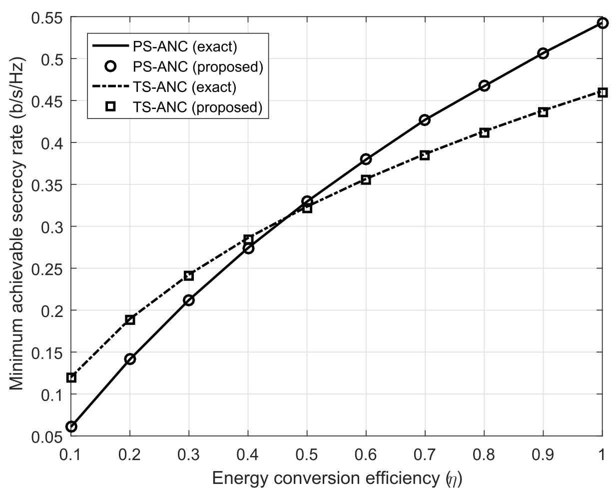

FIGURE 11. **Minimum achievable secrecy rate vs. energy conversion efficiency (η).**

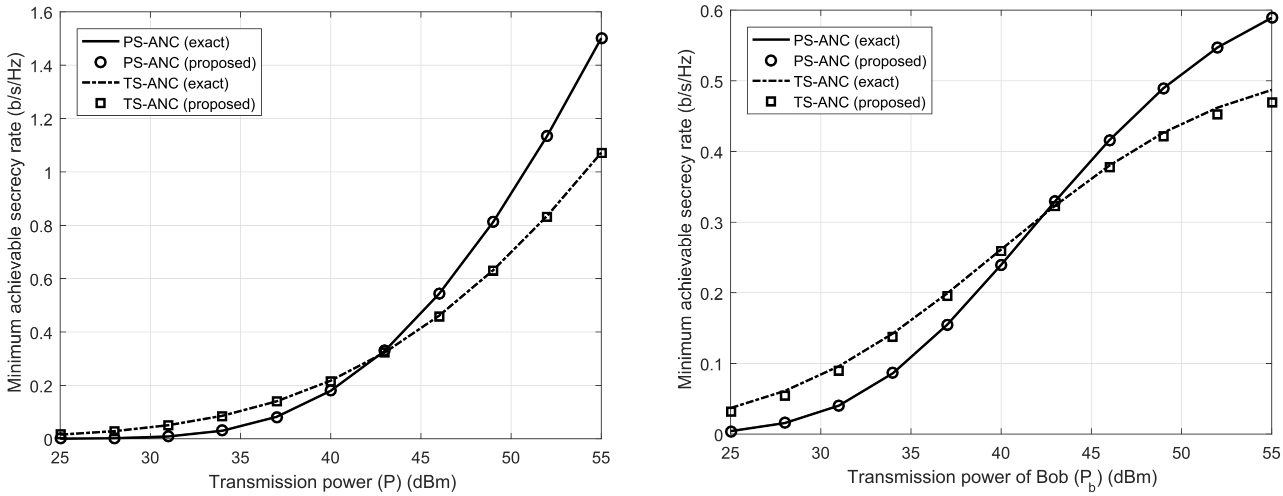

(a) (b)

FIGURE 12. Minimum achievable secrecy rate vs. transmission power (*P*). (a) Power splitting ratio or time switching ratio versus transmit SNR. (b) Minimum achievable secrecy rate versus transmit SNR.

$S_{\min}$ regardless of K. From (27), α^* is decided according to the relationship between α_j^* and α_0^*. In most cases in our simulations, the condition $(\alpha_a^* - \alpha_0^*)(\alpha_b^* - \alpha_0^*) > 0$ is satisfied, so α_j^* rather than α_0^* is chosen as α^*. From Lemma 1, α_j^* is not influenced by h_i in the high SNR environment and thus α^* is fixed at 0.93 in the result. Similar to the PS-ANC, the TS-ANC has a constant β^*, which is unaffected by h_i based on (44), and here β^* is fixed as 0.31. Therefore, $S_{\min}$ has a constant value regardless of the location of eavesdroppers. These behaviors make the proposed protocols more practical because neither the locations nor the number of eavesdroppers are generally known in a real environment.

Figure 8 shows the minimum achievable secrecy rate versus the distance between Alice and Bob (d_{ab}) when the relay is located at the center of d_{ab}. As d_{ab} increases, the signal between Alice and Bob is attenuated seriously, and therefore the $S_{\min}$ of the two protocols deteriorates. The result shows that PS-ANC achieves a higher $S_{\min}$ than TS-ANC when $d_{ab} < 500$ m. In other words, PS-ANC is superior to TS-ANC when Alice is close to Bob.

Figure 9 shows the minimum achievable secrecy rate versus the distance between Alice and relay (d_a) when d_{ab} is fixed at 500 m. As shown, the imbalance between S_a and S_b is serious when the relay is closer to Alice or Bob, which deteriorates $S_{\min}$. Therefore, both PS-ANC and TS-ANC maximize $S_{\min}$ when the relay is located at the center of d_{ab}. In this symmetric case (i.e., $d_a = d_b$), PS-ANC slightly outperforms TS-ANC.

2) EFFECTS OF OTHER FACTORS

Additionally, we study the influences of other factors on the performances of PS-ANC and TS-ANC, e.g., path-loss exponent (m), energy conversion efficiency (η), and transmission power (P). To exclude the effect of the wireless channel, we set $d_{ab} = 500$ m and $d_a = d_b = 250$ m for the following simulations.

Figure 10 shows the minimum achievable secrecy rate versus the path-loss exponent (m). A large m results in a degradation in $S_{\min}$ for both PS-ANC and TS-ANC because of the severe signal attenuation. In addition, we can confirm that the $S_{\min}$ of TS-ANC becomes larger than that of PS-ANC when m is larger than 2.7.

Figure 11 shows the minimum achievable secrecy rate versus the energy conversion efficiency (η). As η increases, the relay can harvest much more energy from the user signals. This allows the relay to use a higher power to forward the relaying signal to the users. In consequence, the $S_{\min}$ of both protocols increases. We also find that the $S_{\min}$ of PS-ANC exceeds that of TS-ANC when η is larger than 0.5.

Figure 12 shows the minimum achievable secrecy rate versus the transmission power (P). Figure 12(a) is the result when Alice and Bob use the same transmission power ($P_a = P_b = P = 43$ dBm) while Figure 12(b) is the result when the transmission power of Alice is fixed at $P_a = 43$ dBm while that of Bob is changed from 14 dBm to 50 dBm. In Figure 12(a), as P increases, both users can receive a stronger signal from the other user but the eavesdroppers are disturbed by both stronger user signals. As a result, the $S_{\min}$ of PS-ANC and TS-ANC improves with increasing P. In In Figure 12(b), as P_b increases, not only Alice receives stronger signal from Bob, but the eavesdroppers are able to overhear the signal from Bob. In consequence, the increasing rate of $S_{\min}$ is smaller than that in Figure 12(a). Moreover, TS-ANC achieves higher $S_{\min}$ than PS-ANC when the transmission power is smaller than 43 dBm for both cases.

VI. CONCLUSIONS

In this paper, we investigated secure ANC protocols with EH in the existence of multiple eavesdroppers. We suggested PS-ANC and TS-ANC that optimize the power splitting ratio (α) and time switching ratio (β), respectively. We showed that the secrecy rate for each user is concave with respect to α and β under the assumption of high SNR and derived optimal α^* and β^* to maximize the minimum achievable secrecy rate ($S_{\min}$). Analysis and simulation results confirmed that PS-ANC and TS-ANC protocols using optimal α^* and β^* maximize $S_{\min}$ and both α^* and β^* depend only on the channel information between the two users and the relay, regardless of the channel information for the eavesdroppers. In addition, comparison of PS-ANC and TS-ANC showed the consistent trend that PS-ANC has the advantage over TS-ANC when the network conditions are unfavorable for eavesdroppers to wiretap (i.e, smaller distance between the two users, symmetric relay position, smaller path-loss exponent, higher energy conversion efficiency, and greater transmission power), and vice versa. Therefore, the proposed PS-ANC and TS-ANC can be used complementarily according to given channel conditions and system parameters.

REFERENCES

[1] S. Katti, R. S. Gollakota, and D. Katabi, "Embracing wireless interference: Analog network coding," in *Proc. ACM SIGCOMM*, 2007, pp. 397–408.

[2] A. Naeem, M. H. Rehmani, Y. Saleem, I. Rashid, and N. Crespi, "Network coding in cognitive radio networks: A comprehensive survey," *IEEE Commun. Surveys Tuts.*, vol. 19, no. 3, pp. 1945–1973, 3rd Quart., 2017.

[3] F. Jameel, S. Wyne, G. Kaddoum, and T. Q. Duong, "A comprehensive survey on cooperative relaying and jamming strategies for physical layer security," *IEEE Commun. Surveys Tuts.*, to be published, doi: 10.1109/COMST.2018.2865607.

[4] Y. Zhang, Y. Gao, B. Yang, and N. Sha, "Analyzing the physical layer security performance of the ANC system," in *Proc. Electron. Instrum. Inf. Syst. (EIIS)*, Jun. 2017, pp. 1–5.

[5] A. Sunny, S. Sarma, and J. Kuri, "Secure transmission in cooperative networks with weak eavesdroppers," *IEEE Signal Process. Lett.*, vol. 22, no. 10, pp. 1693–1697, Oct. 2015.

[6] D. Deng, Z. L. Yang, and M. Zhao, "PHY security enhancement in analog network coding based on artificial noise," in *Proc. Wireless Commun. Signal Process. (WCSP)*, Oct. 2014, pp. 1–6.

[7] H.-M. Wang, Q. Yin, and X.-G. Xia, "Improving the physical-layer security of wireless two-way relaying via analog network coding," in *Proc. Global Telecommun. Conf. (GLOBECOM)*, Dec. 2011, pp. 1–6.

[8] H.-M. Wang, Q. Yin, and X.-G. Xia, "Distributed beamforming for physical-layer security of two-way relay networks," *IEEE Trans. Signal Process.*, vol. 60, no. 7, pp. 3532–3545, Jul. 2012.

[9] K.-H. Liu and P. Lin, "Toward self-sustainable cooperative relays: State of the art and the future," *IEEE Commun. Mag.*, vol. 53, no. 6, pp. 56–62, Jun. 2015.

[10] W. Guo, S. Zhou, Y. Chen, S. Wang, X. Chu, and Z. Niu, "Simultaneous information and energy flow for IoT relay systems with crowd harvesting," *IEEE Commun. Mag.*, vol. 54, no. 11, pp. 143–149, Nov. 2016.

[11] A. A. Nasir, X. Zhou, S. Durrani, and R. A. Kennedy, "Relaying protocols for wireless energy harvesting and information processing," *IEEE Trans. Wireless Commun.*, vol. 12, no. 7, pp. 3622–3636, Jul. 2013.

[12] Z. Chen, B. Xia, and H. Liu, "Wireless information and power transfer in two-way amplify-and-forward relaying channels," in *Proc. IEEE Global Conf. Signal Inf. Process. (GlobalSIP)*, Dec. 2014, pp. 168–172.

[13] K. Tutuncuoglu, B. Varan, and A. Yener, "Throughput maximization for two-way relay channels with energy harvesting nodes: The impact of relaying strategies," *IEEE Trans. Commun.*, vol. 63, no. 6, pp. 2081–2093, Jun. 2015.

[14] Z. Fang, X. Yuan, and X. Wang, "Distributed energy beamforming for simultaneous wireless information and power transfer in the two-way relay channel," *IEEE Signal Process. Lett.*, vol. 22, no. 6, pp. 656–660, Jun. 2015.

[15] M. Ju, J. H. Oh, and K.-S. Hwang, "PSR-based ANC protocol in energy harvesting bidirectional networks," in *Proc. Int. Conf. Ubiquitous Future Netw. (ICUFN)*, Jul. 2016, pp. 187–191.

[16] S. Modem and S. Prakriya, "Performance of analog network coding based two-way EH relay with beamforming," *IEEE Trans. Commun.*, vol. 65, no. 4, pp. 1518–1535, Apr. 2017.

[17] K. Lee, J.-P. Hong, H.-H. Choi, and M. Levorato, "Adaptive wireless-powered relaying schemes with cooperative jamming for two-hop secure communication," *IEEE Internet Things J.*, vol. 5, no. 4, pp. 2793–2803, Aug. 2018.

[18] K. Lee, J.-P. Hong, H.-H. Choi, and T. Q. S. Quek, "Wireless-powered two-way relaying protocols for optimizing physical layer security," *IEEE Trans. Inf. Forensics Security*, vol. 14, no. 1, pp. 162–174, Jan. 2019.

[19] V. N. Q. Bao, N. Linh-Trung, and M. Debbah, "Relay selection schemes for dual-hop networks under security constraints with multiple eavesdroppers," *IEEE Trans. Wireless Commun.*, vol. 12, no. 12, pp. 6076–6085, Dec. 2013.

[20] Y. Yang, Q. Li, W.-K. Ma, J. Ge, and P. C. Ching, "Cooperative secure beamforming for AF relay networks with multiple eavesdroppers," *IEEE Signal Process. Lett.*, vol. 20, no. 1, pp. 35–38, Jan. 2013.

[21] J. Chen, R. Zhang, L. Song, Z. Han, and B. Jiao, "Joint relay and jammer selection for secure two-way relay networks," *IEEE Trans. Inf. Forensics Security*, vol. 7, no. 1, pp. 310–320, Feb. 2012.

[22] L. Liu, R. Zhang, and K.-C. Chua, "Wireless information and power transfer: A dynamic power splitting approach," *IEEE Trans. Commun.*, vol. 61, no. 9, pp. 3990–4001, Sep. 2013.

[23] L. Liu, R. Zhang, and K.-C. Chua, "Wireless information transfer with opportunistic energy harvesting," *IEEE Trans. Wireless Commun.*, vol. 12, no. 1, pp. 288–300, Jan. 2013.

[24] Z. Ding, Z. Ma, and P. Fan, "Asymptotic studies for the impact of antenna selection on secure two-way relaying communications with artificial noise," *IEEE Trans. Wireless Commun.*, vol. 13, no. 4, pp. 2189–2203, Apr. 2014.

[25] J. Mo, M. Tao, Y. Liu, and R. Wang, "Secure beamforming for MIMO two-way communications with an untrusted relay," *IEEE Trans. Signal Process.*, vol. 62, no. 9, pp. 2185–2199, May 2014.

[26] J. Huang and A. L. Swindlehurst, "Joint transmit design and node selection for one-way and two-way untrusted relay channels," in *Proc. Asilomar Conf. Signals, Syst. Comput.*, Nov. 2013, pp. 1555–1559.

[27] M. Stoopman, S. Keyrouz, H. J. Visser, K. Philips, and W. A. Serdijn, "Co-design of a CMOS rectifier and small loop antenna for highly sensitive RF energy harvesters," *IEEE J. Solid-State Circuits*, vol. 49, no. 3, pp. 622–634, Mar. 2014.

[28] X. Lu, P. Wang, D. Niyato, D. I. Kim, and Z. Han, "Wireless networks with RF energy harvesting: A contemporary survey," *IEEE Commun. Surveys Tuts.*, vol. 17, no. 2, pp. 757–789, 2nd Quart., 2015.

[29] A. A. Nasir, X. Zhou, S. Durrani, and R. A. Kennedy, "Wireless-powered relays in cooperative communications: Time-switching relaying protocols and throughput analysis," *IEEE Trans. Commun.*, vol. 63, no. 5, pp. 1607–1622, May 2015.

[30] H. Meyr, M. Moeneclaey, and S. A. Fechtel, *Digital Communication Receivers: Synchronization, Channel Estimation, and Signal Processing* (Wiley Series in Telecommunications and Signal Processing), J. G. Proakis, Ed. Hoboken, NJ, USA: Wiley, 1998.

KISONG LEE (S'10–M'14) received the B.S. degree from the Department of Electrical Engineering, Information and Communications University, South Korea, in 2007, and the M.S. and Ph.D. degrees from the Department of Electrical Engineering, Korea Advanced Institute of Science and Technology, South Korea, in 2009 and 2013, respectively. From 2013 to 2015, he was a Researcher with the Electronics and Telecommunications Research Institute. From 2015 to 2017, he was an Assistant Professor with the Department of Information and Telecommunication Engineering, Kunsan National University. He is currently an Assistant Professor with the School of Information and Communication Engineering, Chungbuk National University, Cheongju, South Korea. His research interests include self-organizing networks, radio resource management, magnetic induction communication, wireless power transfer, and energy harvesting networks.

HYUN-HO CHOI (S'02–M'07) received the B.S., M.S., and Ph.D. degrees from the Department of Electrical Engineering, Korea Advanced Institute of Science and Technology, South Korea, in 2001, 2003, and 2007, respectively. From 2007 to 2011, he was a Senior Engineer with the Communication Laboratory, Samsung Advanced Institute of Technology (SAIT), South Korea. Since 2011, he has been a Professor with the Department of Electrical, Electronic, and Control Engineering, Institute for Information Technology Convergence, Hankyong National University, South Korea. His current research interests include bio-inspired algorithms, distributed optimization, machine learning, wireless energy harvesting, mobile ad hoc networks, and the next-generation wireless communication. He is a member of IEICE, KICS, and KIICE. He was a co-recipient of the SAIT Patent Award in 2010 and the Paper Award at the Samsung Conference in 2010. He received the Excellent Paper Award at ICUFN 2012, the Best Paper Award at ICN 2014, and the Best Paper Award at Qshine 2016.